AIMS Materials Science, 7(3): 312–322.
DOI: 10.3934/matersci.2020.3.312
Received: 26 March 2020
Accepted: 05 June 2020
Published: 11 June 2020

http://www.aimspress.com/journal/Materials

Research article

Transformation superplasticity of laminated $CuAl_{10}Fe_3Mn_2$ bronze-intermetallics composites

Marek Konieczny*

Department of Metals Science and Materials Technologies, Kielce University of Technology, Kielce, Poland

* **Correspondence:** Email: mkon@tu.kielce.pl; Tel: +48413424321.

Abstract: The tensile properties at elevated temperatures (780, 800 and 820 °C) for the laminated $CuAl_{10}Fe_3Mn_2$-intermetallics composites have been investigated. The bronze-intermetallics laminated composites were transformation superplastic at 800 °C. When the initial strain-rate was 0.7×10^{-3} s^{-1} fracture elongation of 455% was achieved. An excursion through the transformation range α→β and back β→α resulted in a finite, irreversible strain increment on each thermal cycle. These strains were accumulated without fracture of intermetallic layers. A small amount of cavities were formed during superplastic deformation of aluminum bronze which were nucleated at the iron-rich particles and grew along the force axis. At 780 and 820 °C, the expected superplastic behavior of laminated composites was not realized because α and β phase grains were too coarse to allow deformation by grain-boundary sliding through microstructural superplasticity and cracking in the intermetallic layers began.

Keywords: aluminum bronze; intermetallics; laminated composite; transformation superplasticity; mechanical properties

1. Introduction

Since over three decades there has been significant interest in the fabrication and thorough investigation of a variety of laminated metal composites [1]. Very interesting and potentially useful

are metal-intermetallic (MIL) composites that can perform various functions, such as blast mitigation, heat exchange and vibration damping, wherein lamination normally improves fracture toughness and fatigue behavior [2,3]. It is beneficial that MIL composites can be easily produced using bonding techniques between metal foils where the size and the number of layers are not limited [4]. These composites combine the ductility and toughness of metals with the higher strength and lower density which is characteristic feature for intermetallics. Previous works revealed that Cu-intermetallic and aluminum bronze-intermetallic composites can be easily produced by reaction synthesis that occurs at the interface of copper or bronze and titanium [5–8]. It was also shown [7] that at 700 °C a failure of the Cu-intermetallics tensile tested samples was not followed by rapid cracking of intermetallics layers due to their plasticization. Superplasticity is defined as the capability of a polycrystalline material to display extremely high tensile ductility prior to failure [9]. In a very broad classification, superplasticity is divided into two classes: (1) structural superplasticity, which originates from fine grain size, and (2) transformational superplasticity, which originates from phase transformation and is applicable to titanium alloys [10,11] or iron and steels [12]. Transformation superplasticity has significant potential as a cost-effective shaping process for composites (e.g. Ti–6Al–4V/TiC_p) and intermetallics (e.g. Ti_3Al) [10]. Greenwood and Johnson [13] proposed a widely accepted model of transformation superplasticity which has no grain-size requirement because it relies on the biasing of internal stresses produced by cyclical phase transformation. Previous studies have pointed that a non-superplastic materials could be made superplastic by lamination with the micrograin aluminum bronze that is a superplastic material [1,14,15]. Aluminum bronzes are commonly used corrosion-resistant alloys of copper. They usually contain from 4 to 15 wt% aluminum and small amounts of other metals. Alloys containing from 9 to 12 wt% aluminum are often fabricated by gravity diecasting and sand casting into many machine parts or tools and ship propellers [16]. Above 565 °C [17], the microstructure of alloys with 9.4 to 11.8 wt% aluminum consists of two phases with differing proportions of α and γ_2 grains (Figure 1).

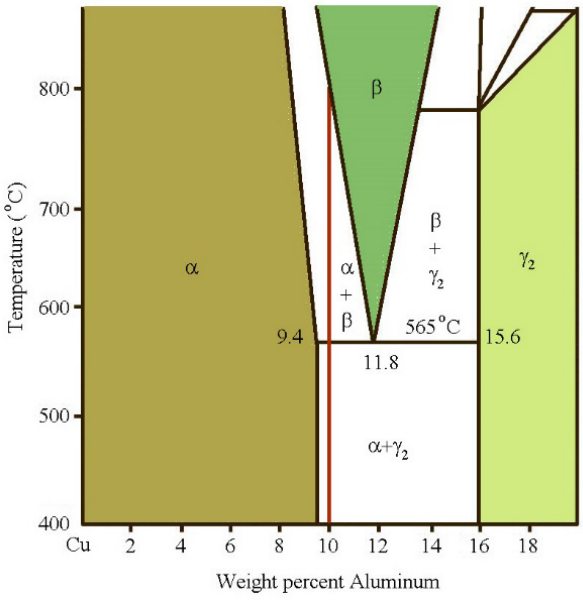

Figure 1. Part of the Cu–Al binary phase diagram from copper side.

The purpose of the article is to recognize the effect of high temperature on the possibility of superplastic behavior and demonstrate that transformation superplasticity can be achieved in laminated $CuAl_{10}Fe_3Mn_2$ bronze-intermetallics composites which opens the possibility to form objects into complicated shapes.

2. Materials and methods

For bronze-intermetallics laminated composites fabrication 0.05 mm thick titanium foils were alternatively stacked between $CuAl_{10}Fe_3Mn_2$ foils of 0.3 mm thickness that were produced from 2.5 mm thick sheet by hot rolling. The chemical composition (at%) of as-received CP-titanium was 99.51 Ti, 0.09 Fe, 0.08 C, 0.07 Al, 0.18 O, 0.05 V and 0.02 N. The chemical composition (at%) of aluminum bronze was 10.75 Al, 2.78 Fe, 1.98 Mn, 0.76 Ni, 0.29 Zn, 0.08 Sn and balanced Cu. Foils were cut into 60 × 18 mm rectangular pieces. Any present contamination was removed in a bath of 5% HF in water. After rinsing in water, foils were stacked into laminates in an alternating sequence (6 layers of aluminum bronze and 5 of Ti). A pressure of 5 MPa was employed at room temperature in a specially constructed vacuum furnace to ensure good contact between foils (Figure 2).

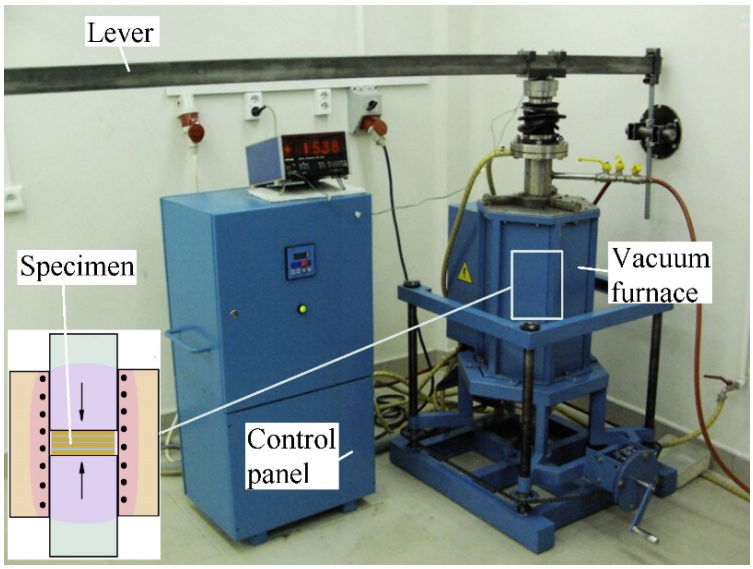

Figure 2. Vacuum furnace used to fabricate laminated composites.

Previous experiments shown [8,18] that a temperature of at least 870 °C was necessary for the start and rapid development of structural processes at the interface between aluminum bronze and titanium. The temperature was increased from 20 to 600 °C at a heating rate of 0.25 °C/s. The samples were heated in vacuum of 0.01 Pa at 800 °C for 1h under applied 5 MPa pressure to allow diffusion bonding of the layers. After that the pressure was removed and the specimens were reheated to 875 °C and held at this temperature for 1h. The temperature was then decreased slowly (cooling rate of 0.16 °C/s) to 600 °C and the pressure of 5 MPa was applied again. Finally, the samples were furnace-cooled to room temperature (Figure 3).

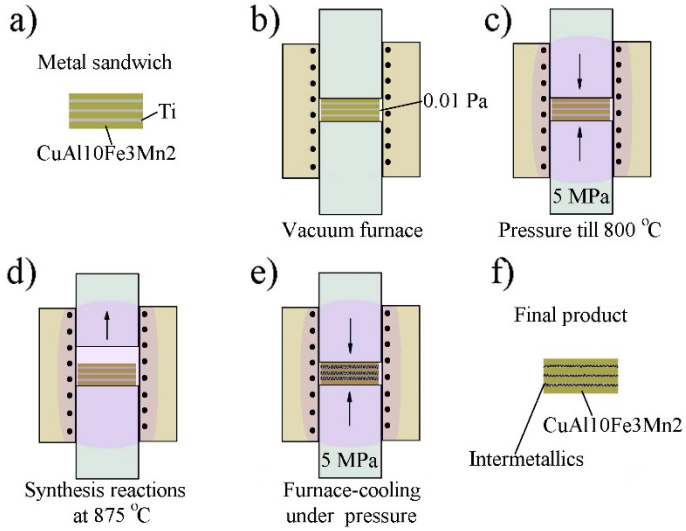

Figure 3. A schematic diagram of consecutive steps (a–f) during fabrication of laminated bronze-intermetallics composite.

Flat specimens of 12 mm gauge length, 6 mm gauge width and 2.2 mm thickness were machined from fabricated laminated materials and, for comparison, from aluminum bronze. Tensile tests were carried out in air at elevated temperatures (780, 800 and 820 °C) at a nominal strain-rate of 0.7×10^{-3} s^{-1}, on Amsler testing machine fitted with a vertical split tube furnace. After mounting the specimen, the furnace was heated to the testing temperature in about 0.5 h and held at that temperature for another 0.5 h before starting deformation. Temperatures along the gauge length of specimens were maintained within ±5 °C of the test temperature. The strain-rate sensitivity (m) for laminated composites and aluminum bronze was appointed by determining the tangential slope of log stress versus log strain-rate curves. Thermal analysis was carried out in argon using a TG-DSC Setaram device. The samples for metallographic investigations were cut using diamond blade and polished applying standard techniques. Microstructural observations were performed using a JEOL JMS 5400 scanning electron microscope (SEM) and a Nikon ECLIPSE MA 200 optical microscope (OM). The lateral linear distribution of elements content and chemical composition of the phases was determined by an energy dispersive spectroscopy utilizing a ISIS 300 Oxford Instruments. Before the samples were examined with the optical microscope they had been etched to reveal grain boundaries and the structure of the intermetallic layers. Etching was performed with solution of 40 g CrO_3, 7.5 g NH_4Cl, 8 mL H_2SO_4, 50 mL HNO_3 and 1900 mL H_2O. Vickers measurements were performed by Matsuzawa microhardness tester (loads of 0.981 N were applied for 15 s).

3. Results and discussion

The fabricated layered materials were well-bonded and almost fully dense (Figure 4).

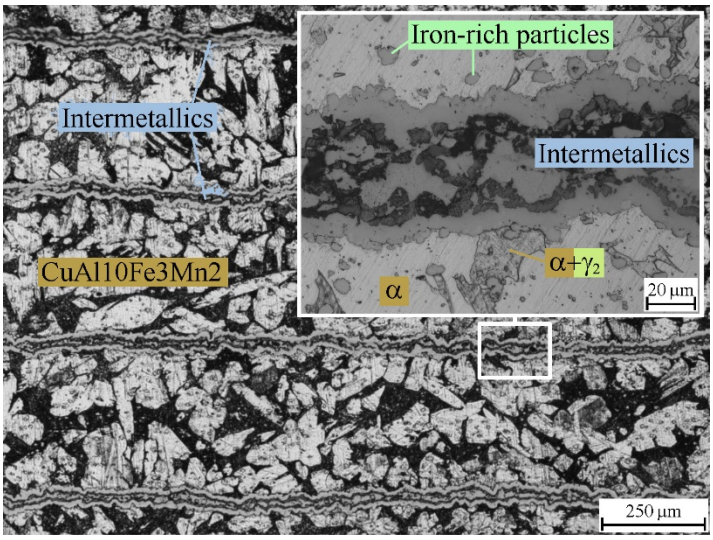

Figure 4. Microstructure of the as-produced laminated composite (OM and SEM).

Previously published results [6,18] showed that the predominant part of the intermetallic layers were $TiCu_2Al$ and TiCuAl phases with a very small content of Ti_2Cu (Figure 5).

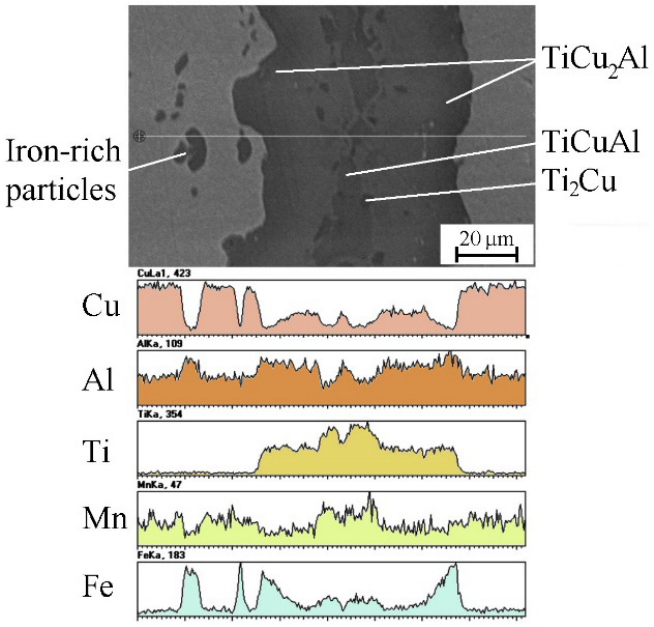

Figure 5. Microstructure of the intermetallic layer in composite together with the lateral linear distribution of elements content (SEM).

Lazurenko et al. [19] based on the results obtained by in-situ synchrotron X-ray diffraction, suggested that formation of the TiCuAl phase inevitably accompanies the formation of other phases from the ternary Ti–Al–Cu system. The maximum hardness values in the range of 660 to 770 HV were achieved at the bronze/intermetallic interface due to the presence of the $TiCu_2Al$ phase. For the mixture of TiCuAl and Ti_2Cu phases hardness was in the range of 510 to 550 HV. The values of

hardness for aluminum bronze were in the range of 210 to 260 HV and were over two times lower than for the intermetallic layers. Of interest in the present investigation is that transformation superplasticity was observed in the $CuAl_{10}Fe_3Mn_2$ alloy which has hypoeutectoid composition. The used deformation temperatures (780, 800 and 820 °C) were distinctly higher than the eutectoid temperature (Figure 1). At 780 °C the aluminum bronze was in the two phase α + β field with a duplex microstructure additionally containing iron-rich particles, that can be seen in the layers of the alloy shown in Figures 4 and 5. At 820 °C the aluminum bronze was in the one phase field β. But at 800 °C (and precisely saying in the temperature range of 795 and 805 °C because measured temperature was systematically changing in time) there was the transformation temperature α→β (Figure 6).

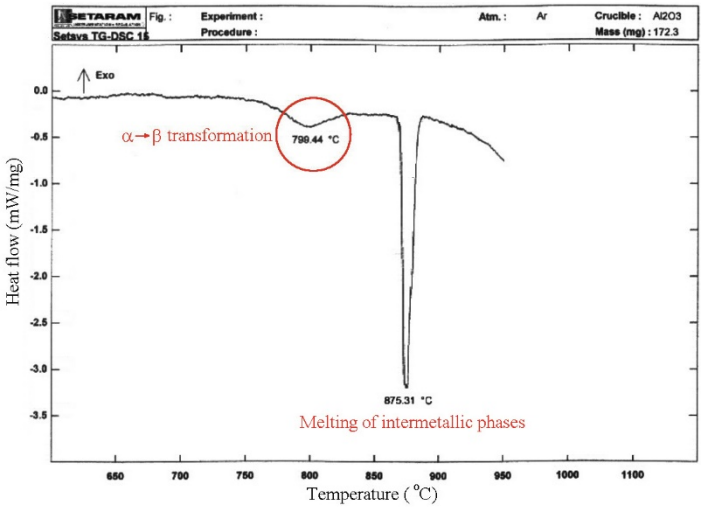

Figure 6. Results of DSC analysis obtained during heating showing α→β transformation temperature.

Previously published results shown [8] that the elongation of laminated composites exhibited at room temperature was rather moderate and reached only 8 % (12 % for $CuAl_{10}Fe_3Mn_2$ bronze). Formation of many cracks in the intermetallic layers was the characteristic trait of the prolonged deformation. With continual increase of the cracks number in intermetallic layers the bronze layers gradually underwent the total external load and as the number and distribution of cracks achieved a critical limit, the final failure took place by shearing fracture of the bronze layers. The characteristic of failure described for the $CuAl_{10}Fe_3Mn_2$-intermetallics composites is thoroughly consistent with previous studies of damage mechanisms in various laminated composites because they behave very similar during tensile testing at room temperature [1–7]. Dunlop and Taplin shown [15] that temperature had significant influence on the ductility of the aluminum bronze. It was also proven [7] that at temperatures higher than 700 °C the Cu-based intermetallics can be deformed plasticly to some extent without their rapid cracking. The effect of investigation temperature on peak values of *m* and elongation of laminated composites as well as of $CuAl_{10}Fe_3Mn_2$ bronze is shown in Table 1.

Table 1. Effect of investigation temperature on peak values of *m* and elongation at fracture.

Temperature (°C)	Peak *m*		Elongation (%)	
	Composite	Bronze	Composite	Bronze
780	0.44	0.56	180	310
800	0.55	0.63	455	780
820	0.46	0.58	210	340

The flow stresses of all obtained tensile stress-strain curves raised instantly to the peak values and then dropped slowly. For laminated composites the drop was constant until failure but for the aluminum bronze the decrease progressed to the state-stage flow before failure (Figure 7).

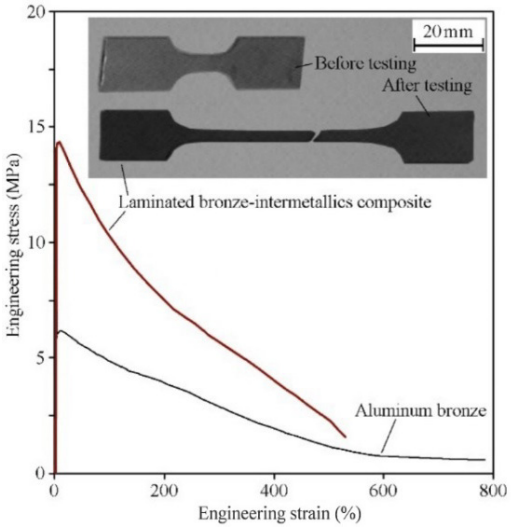

Figure 7. Engineering stress-strain curves for investigated materials deformed at 800 °C at a nominal strain-rate of 0.7×10^{-3} s^{-1}.

The values of peak stresses for the laminated composited were 18, 14.5 and 12 MPa corresponding to the deformation temperature of 780, 800 and 820 °C, respectively. The elongation at the beginning of plastic instability, as specified by the points of peak stresses in the tensile tests, were found to make a relatively slight contribution to the total elongations for both investigated materials (Figure 7). Maximum elongation for a nominal strain-rate of 0.7×10^{-3} s^{-1} for laminated composites and aluminum bronze occurred at 800 °C and was 455 and 780 %, respectively. A similar effect at a strain-rate of 0.65×10^{-3} s^{-1} at 800 °C has been noted by Dunlop and Taplin [15] in aluminum bronze of similar composition but without Mn. In general, materials exhibit the superplasticity when the value of *m* surpass 0.5. As shown in Table 1, at all investigated temperatures the value of *m* for aluminum bronze exceeded 0.5 and was in the range of 0.56 to 0.63. On the other hand, the value of *m* for laminated composites was in the range of 0.44 to 0.55, and exceeded 0.5 only at 800 °C. This phenomenon can be explained by fact that the distribution of phases within the microstructure of aluminum bronze varies with temperature. At 780 °C the aluminum bronze was in the two phase $\alpha + \beta$ field but grains of α phase were too coarse (Figure 4) to allow deformation by grain-boundary sliding through microstructural superplasticity. At 800 °C

(in the temperature range of 795 and 805 °C) occurred transformation α→β during which were created internal stresses due to phase density difference. Nieh et al. [20] shown that internal-stress plasticity is observed in crystalline solids upon generation of internal stresses in the presence of an external stress. The transformation mismatch stresses are biased in the direction of the applied external stress and deformation occurs. Transformation superplasticity has no grain-size requirement because it relies on the biasing of internal stresses produced by cyclical phase transformation [11]. An excursion through the transformation range α→β and back β→α results in a finite, irreversible strain increment on each thermal cycle about the range of 795 and 805 °C. These strains were accumulated without fracture. Evidently, the laminated CuAl10Fe3Mn2-intermetallics composite showed the superplastic ductility only at 800 °C because grains of α and β phases in bronze layers were able to deform gradually together with grains of intermetallic phases (Figure 8).

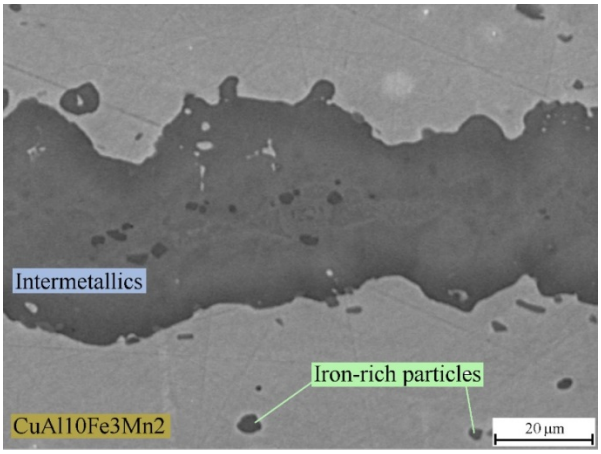

Figure 8. Micrograph of the intermetallic layer deformed at 800 °C (SEM).

At 780 and 820 °C the superplastic behavior of laminated composites was not realized and cracking in the intermetallic layers began (Figure 9).

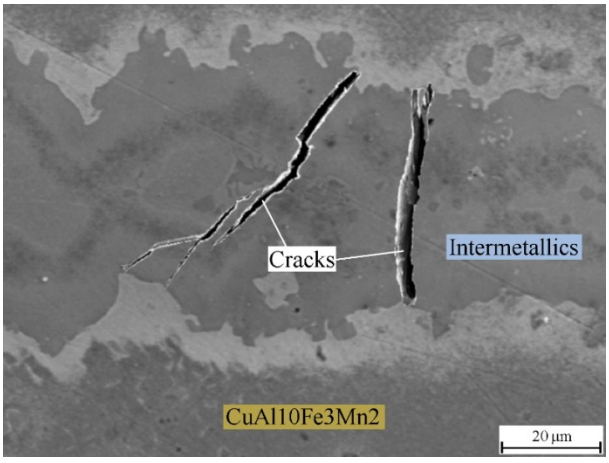

Figure 9. Micrograph of the intermetallic layer deformed at 780 °C (SEM).

When cracks appeared the layers of bronze could still deform but total elongation was about two times smaller than at 800 °C. A similar effect has been reported by Tsai et al. [21] in laminated ultrahigh carbon steel-aluminum bronze composites that have a high strain rate sensitivity exponent *m* at elevated temperatures in the range of 750 to 850 °C.

After deformation to failure at 800 °C, no significant necking occurred at the superplastic fracture of laminated $CuAl_{10}Fe_3Mn_2$-intermetallics composites and the gauge section of tensile specimen became much thinner (Figure 7). The gauge width reduced from 6 to 4.1 mm (32%) and the gauge thickness decreased from 2.2 to 0.73 mm (67%). During superplastic deformation at 800 °C there were not produced cracks in intermetallic layers and their thickness was reduced from about 0.06 mm to about 0.04–0.025 mm (Figures 5 and 8). A small amount of cavities in bronze layers was observed in the microstructure of as-polished gauge section in longitudinal direction. It is worth noting that cavities mainly nucleated at the iron-rich particles in bronze and grew along the force axis (Figure 10).

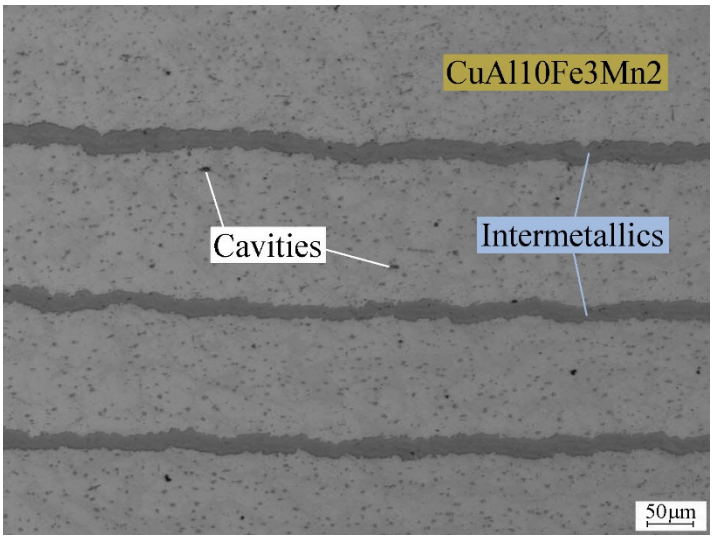

Figure 10. Microstructure of the gauge section of tensile specimen after superplastic deformation at 800 °C (SEM).

4. Conclusions

For the laminated $CuAl_{10}Fe_3Mn_2$-intermetallics composites, the tensile properties at elevated temperatures (780, 800 and 820 °C) have been investigated. From obtained results and discussions, the following conclusions can be drawn:

1. The elongation of laminated composites exhibited at room temperature reaches only 8%. Formation of many cracks in the intermetallic layers is the characteristic feature of the prolonged deformation.
2. $CuAl_{10}Fe_3Mn_2$-intermetallics laminated composites can be made superplastic at 800 °C. Fracture elongation of 455% may be achieved when the initial strain-rate is 0.7×10^{-3} s^{-1}.
3. The value of *m* for laminated composites is in the range of 0.44 to 0.55, and exceeds 0.5 only at around 800 °C.

4. An excursion through the transformation range α→β and back β→α results in a finite, irreversible strain increment on each thermal cycle. These strains are accumulated without fracture of intermetallic layers.
5. At 780 and 820 °C the expected superplastic behavior of laminated composites is not realized because α and β grains are too coarse to allow deformation by grain-boundary sliding through microstructural superplasticity and cracking in the intermetallic layers begins.
6. A small amount of cavities are formed during transformation superplastic deformation of aluminum bronze which are nucleated at the iron-rich particles and grow along the force axis.

Acknowledgments

This research did not receive any specific grant from funding agencies in the public, commercial, or not-for-profit sectors.

Conflict of interests

The author declare no conflict of interests.

References

1. Wadsworth J, Lesuer DR (2000) Ancient and modern laminated composites—from the Great Pyramid of Gizeh to Y2K. *Mater Charact* 45: 289–313.
2. Vecchio KS (2005) Synthetic multifunctional metallic-intermetallic laminated composites. *JOM* 57: 25–31.
3. Bloyer DR, Venkateswara Rao KT, Ritchie RO (1997) Laminated Nb/Nb_3Al composites: Effect of layer thickness on fatigue and fracture behavior. *Mater Sci Eng A-Struct* 239–240: 393–398.
4. Alman D, Dogan CP, Hawk JA, et al. (1995) Processing, structure and properties of metal-intermetallic layered composites. *Mater Sci Eng A-Struct* 192–193: 624–632.
5. Konieczny M, Dziadoń A (2007) Mechanical behavior of multilayer metal-intermetallic laminate composite synthesized by reactive sintering of Cu/Ti foils. *Arch Metall Mater* 52: 555–562.
6. Konieczny M, Dziadoń A (2007) Strain behaviour of copper-intermetallic layered composite. *Mater Sci Eng A-Struct* 460–461: 238–242.
7. Konieczny M (2007) Deformation mechanisms in copper-intermetallic layered composite at elevated temperatures. *Kovove Mater* 45: 313–317.
8. Konieczny M (2019) Mechanical properties of laminated $CuAl_{10}Fe_3Mn_2$ aluminum bronze-intermetallics composites. *IOP Conf Ser-MSE* 461: 012042.
9. Sankaran KK, Mishra RS (2017) Alloy design for advanced manufacturing processes, *Metallurgy and Design of Alloys with Hierarchical Microstructures*, 1 Ed., Elsevier, 407–449.
10. Frary M, Schuh C, Dunand DC (2002) Kinetics of biaxial dome formation by transformation superplasticity of titanium alloys and composites. *Metall Mater Trans A* 33: 1669–1680.

11. Li Q, Chen EY, Bice DR, et al. (2007) Transformation superplasticity of cast titanium and Ti–6Al–4V. *Metall Mater Trans A* 38: 44–51.
12. Marvin JD, Dunand DC (2006) Transformation-mismatch plasticity in sub-millimetre iron wires. *Mater Sci Eng A-Struct* 421: 35–39.
13. Greenwood GW, Johnson RH (1965) The deformation of metals under small stresses during phase transformations. *P Roy Soc A-Math Phy* 283: 403–422.
14. Ridley N, Xiao Guo Z, Higashi K (1990) An experimental investigation of the superplastic forming behavior of a commercial Al-bronze. *Metall Mater Trans A* 21: 2957–2966.
15. Dunlop GL, Taplin DM (1972) The tensile properties of a superplastic aluminium bronze. *J Mater Sci* 7: 84–92.
16. Kaplan M, Yildiz AK (2003) The effects of production methods on the microstructures and mechanical properties of an aluminum bronze. *Mater Lett* 57: 4402–4411.
17. Massalski TB, Murray JL, Bennet LH, et al. (1992) *Binary Alloy Phase Diagrams*, Ohio: ASM International, 3: 82.
18. Konieczny M, Mola R, Kargul M, et al. (2018) Microstructure evolution of laminated aluminum bronze-intermetallics composite. *METAL 2018 Conference Proceedings*, Ostrava: Tanger, 1587–1592.
19. Lazurenko DV, Bataev IA, Mali VI, et al. (2018) Synthesis of metal-intermetallic laminate (MIL) composites with modified Al3Ti structure and in situ synchrotron X-ray diffraction analysis of sintering process. *Mater Design* 151: 8–16.
20. Nieh TG, Wadsworth J, Sherby OD (1997) *Superplasticity in Metals and Ceramics*, Cambridge: Cambridge University Press, 245.
21. Tsai HC, Higashi K, Sherby OD (1993) Superplasticity in an ultrahigh carbon steel-aluminum bronze laminated composite. *Proceedings of the International Conference on Advanced Composite Materials*, 1287–1293.

AIMS Press